Kinetics of β_2-Integrin and L-Selectin Bonding during Neutrophil Aggregation in Shear Flow

Pushkar Tandon and Scott L. Diamond
Institute for Medicine and Engineering, Department of Chemical Engineering, University of Pennsylvania, Philadelphia, Pennsylvania 19104 USA

ABSTRACT Activated neutrophils aggregate in a shear field via bonding of L-selectin to P-selectin glycoprotein ligand-1 (PSGL-1) followed by a more stable bonding of LFA-1 (CD11a/CD18) to intercellular adhesion molecule 3 (ICAM-3) and Mac-1 (CD11b/CD18) to an unknown counter receptor. Assuming that the Mac-1 counter receptor is ICAM-3-like in strength and number, rate processes were deconvoluted from neutrophil homoaggregation data for shear rates (G) of 100–3000 s^{-1} with a two-body hydrodynamic collision model (Tandon and Diamond, 1997. *Biophys. J.* 73:2819–2835). For integrin-mediated aggregation (characteristic bond strength of 5 μdynes) in the absence of L-selectin contributions, an average forward rate of $k_f = 1.57 \times 10^{-12}$ cm^2/s predicted the measured efficiencies for $G = 100–800$ s^{-1}. For a selectin bond formation rate constant equal to the integrin bond formation rate constant, the colloidal stability of unactivated neutrophils was satisfied for a reverse rate of the L-selectin–PGSL bond corresponding to an average bond half-life of 10 ms at a characteristic bond strength of 1 μdyne. Colliding neutrophils initially bridged by at least one L-selectin–PSGL-1 bond were calculated to rotate from 8 to 50 times at $G = 400$ to 3000 s^{-1}, respectively, before obtaining mechanical stability in sheared fluid of either 0.75 or 1.75 cP viscosity. Thus for $G > 400$ s^{-1}, the interaction time needed for the rotating aggregates to become stable was relatively constant at 52.5 $\pm$ 8.5 ms, largely independent of shear rate or shear stress. Aggregation data and the colloidal stability criterion can provide a consistent set of forward and reverse rate constants and characteristic bond strengths for a known time-dependent stoichiometry of receptors on cells interacting in a shear flow field.

NOMENCLATURE

A	mobility function along line of centers of the particles
A_0	initial contact area
A_{coll}	swept collision area
a_1, a_2	radii of the colliding particles
B	mobility function normal to the line of the centers of the colliding particles
C	correction to Stokes' law taking into account presence of second sphere
D_i	diffusion constant of receptors on the membrane
G	shear rate
f_c	characteristic bond strength
F_A	van der Waals attractive force
F_R	electrostatic repulsion force
F_{drag}	drag force
k_f	forward rate of bond formation
k_r	reverse rate of bond formation
N_i	number density of aggregates of size class i
N_b	bonds per unit area
N_{crit}	critical number of bonds needed to hold aggregate together
N_{rec}	number of receptors per unit area
v	volume
V_{eff}	relative velocity between the aggregates
s	dimensionless distance between the aggregates
t	time
t^*	dimensionless time
T_i	interaction time

Greek letters

$\beta(i, j)$	collision frequency between particles of size classes i and j
β_G	Smoluchowski collision frequency
ϵ	collision efficiency (empirical)
ϵ_h	hydrodynamic collision efficiency
ϵ_{r+h}	overall collision efficiency (including hydrodynamic and receptor effects)
$\bar{\epsilon}$	time-averaged collision efficiency
η	effectiveness factor
λ	size ratio of the colliding aggregates
τ	collision time
τ_{rot}	time of rotation
ξ	dimensionless separation distance between the colliding aggregates

INTRODUCTION

At sites of inflammation, neutrophils roll on the endothelium and subsequently develop firm adhesions before their migration out of the vascular space. Neutrophils adherent to the endothelium can mediate the capture of neutrophils flowing near the vessel wall (Bargatze et al., 1994). Furthermore, free flowing homoaggregates of neutrophils and heteroaggregates of platelets and neutrophils may participate in certain cardiovascular disorders. Several recent studies have defined the receptor mechanisms that support neu-

Received for publication 8 May 1998 and in final form 25 August 1998.
Address reprint requests to Dr. Scott L. Diamond, Department of Chemical Engineering, Institute for Medicine and Engineering, University of Pennsylvania, 394 Towne Building, 220 S. 33rd St., Philadelphia, PA 19104. Tel.: 215-898-8652; Fax: 215-573-2093; E-mail: sld@seas.upenn.edu.

0006-3495/98/12/3163/16 $2.00

trophil homoaggregation (Taylor et al., 1996; Walchek et al., 1996; Okuyama et al., 1996; Guyer et al., 1996). LFA-1 (CD11a/CD18) binding to intercellular adhesion molecule 3 (ICAM-3) as well as Mac-1 (CD11b/CD18) binding to an unknown receptor can facilitate integrin-mediated homoaggregation without L-selectin at shear rates below 400 s^{-1}. Below 100 s^{-1}, the role of L-selectin–PSGL-1 binding is minor, because little inhibition of aggregation was observed with blocking Fab against L-selectin at this shear rate (Taylor et al., 1996).

Neutrophils present L-selectin on the tips of the microvilli. Both L-selectin and ICAM-3 are released from the cell surface after neutrophil activation on the time scale of minutes (Taylor et al., 1996; del Pozo et al., 1994). Mac-1 and LFA-1 are not active on the resting neutrophil surface. Upon activation, Mac-1 and LFA-1 antigenic levels increase dramatically to ~150,000 Mac-1/cell and ~40,000 LFA-1/cell. Only ~10% of this antigen is considered to be active (Diamond and Springer, 1993). Moreover, the binding avidity of active Mac-1 and LFA-1 may undergo some down-regulation at later times.

For experiments conducted at a defined shear rate, the measured collision efficiency, ϵ, based on fMLP-induced aggregation over the first 30 s for purely integrin-mediated neutrophil homoaggregation (anti-L-selectin Fab present), drops nearly 100-fold as the shear rate increases from 100 to 800 s^{-1}. The collision efficiency is a ratio of the number of successful collisions/number of total collisions predicted by Smoluchowski collision theory. Integrins alone appear to be insufficient to mediate aggregation above 400 s^{-1} when L-selectin plays an important role in facilitating aggregation of fMLP-stimulated neutrophils (Taylor et al., 1996). Interestingly, the value of ϵ goes through a maximum at $G = 400$ s^{-1}. This is consistent with observations of CD62P,E,L-mediated rolling displaying a maximum with shear stress presumably due to stress-mediated delivery of microvilli to the rolling contact area or torque enhancement of bonding (Finger et al., 1996; Lawrence et al., 1997). High-resolution, high-speed imaging of the rolling contact area or the collisional contact area in shear flow has not been reported.

In the present study, we calculate the collision efficiency ϵ, an empirically determined parameter in the studies of Taylor et al. (1996), by systematically taking into account effects due to hydrodynamics and receptor interactions. The hydrodynamic effect on the collision frequency is calculated by considering neutrophils and their aggregates as solid spheres and performing trajectory calculations to obtain the far-upstream cross-section area. Particle flux through this cross section allows prediction of the particle collision frequency. Particles in collision with other particles, caused by the shear fluid flow, are bound together if enough time is available for formation of integrin and selectin bonds. The successful collision frequency, including both receptor and hydrodynamic effects, has been included in a population balance framework to predict the size evolution of the neutrophil aggregate population.

This approach allowed deconvolution from the aggregation data of fundamental rate constants for receptor bonding interactions that have time-dependent stoichiometry. The method provides a tool for the study of the rate of bond formation as it is influenced by receptor number and prevailing hydrodynamic forces during bond formation. Cell aggregation studies conducted in a viscometer allow the probing of interactions on a millisecond time scale that is well suited for understanding selectin and integrin bond dynamics.

THEORY

Collision efficiencies

We have used the methods developed by Tandon and Diamond (1997) to estimate the neutrophil collision efficiency, including both receptor and hydrodynamic receptor interaction effects, for a given combination of shear rate, fluid viscosity, and time-dependent receptor numbers (LFA-1, Mac-1, L-selectin, PSGL-1, ICAM-3). The overall collision efficiency, ϵ_{r+h}, is the ratio of successful collisions relative to the number of collisions estimated by the Smoluchowski equation for linear trajectories without viscous interactions. Using linear trajectory analysis, Smoluchowski (1917) defined, for the collision frequency for two spheres of volume u and v (or radii a_1 and a_2) undergoing shear-induced aggregation,

$$\beta_G(u, v) = \frac{G}{\pi}[u^{1/3} + v^{1/3}]^3 \quad \text{or} \quad \beta_G = \frac{4G}{3}[a_1 + a_2]^3 \qquad (1a)$$

where G is the shear rate. We present methods to systematically predict the collision efficiency ϵ_{r+h}, which is an empirically determined premultiplier of β_G that fits the aggregation data (Bell et al., 1989a,b; Huang and Hellums, 1993a,b,c; Taylor et al., 1996; Belval and Hellums, 1986; Neelamegham et al., 1997). The empirically determined efficiency ϵ, either the instantaneous or time-averaged value $\bar{\epsilon}$, includes effects of both shear flow hydrodynamics and neutrophil receptor biology. To delineate the effects of hydrodynamics and receptor binding on the population dynamics, a modified collision kernel is defined as

$$\beta = \epsilon_{r+h}\beta_G = \epsilon_r\epsilon_h\beta_G \qquad (1b)$$

where ϵ_h is the hydrodynamic collision efficiency and ϵ_r is the receptor binding efficiency. The product $\epsilon_h\beta_G$ gives the actual collision frequency, considering detailed flow fields around the colliding spherical particles. ϵ_r represents the fraction of actual collisions ($\epsilon_h\beta_G$) that results in receptor binding leading to successful aggregation of the colliding particles. The successful collision kernel, $\beta(u, v)$, is used in a population balance equation (PBE) to predict the evolution of number densities of particles of different sizes. The PBE defines the rate of change of number density, N_i, of

neutrophil aggregates comprising i singlets and is given as

$$\frac{\partial N_i}{\partial t} = \frac{1}{2}\sum_{j=1}^{i-1} \beta(j, i-j) N_j N_{i-j} - N_i \sum_{j=1}^{\infty} \beta(i, j) N_j \quad (1c)$$

where $\beta(i, j)$ is the successful collision frequency between aggregates comprising i and j singlets, respectively. The first term on the right-hand side (RHS) of Eq. 1c represents the birth of particles with i singlets by aggregation of particles having fewer than i singlets (the factor $\frac{1}{2}$ prevents double counting). The second term of the RHS is associated with the death of the particles with i singlets as a result of their aggregation with other particles to form even larger particles. Integration of Eq. 1c by the Runge-Kutta-Mercer method with appropriate initial conditions yields the evolution of aggregate number density distribution with time. Disaggregation of stable aggregates is not considered.

For our calculations, we consider the radius of a neutrophil singlet to be 3.75 μm. The distance that the aggregates must approach each other for a collision to occur is dictated by the neutrophil surface roughness and is estimated to be 400 nm (average length of the neutrophil microvilli). For a spherical coordinate (r, θ, ϕ) system, the relative trajectory of two spherical particles of arbitrary radii a_1 and a_2 ($\lambda = a_2/a_1$, $\lambda \leq 1$) in a shear field of strength G ($V_x = Gy$) (Fig. 1 *A*) is described by the equations (Batchelor and Green, 1972; Zeichner and Schowalter, 1977; Adler, 1981a,b; Van de Ven, 1989; Wang et al., 1994; Tandon and Diamond, 1997)

$$\frac{ds}{dt^*} = s[1 - A(\xi, \lambda)]\sin^2\theta \sin\phi \cos\phi + \frac{C(\xi, \lambda)(F_A + F_R)}{3\pi\mu a_1^2 G(1+\lambda)}$$

$$\frac{d\theta}{dt^*} = [1 - B(\xi, \lambda)]\sin\theta \cos\theta \sin\phi \cos\phi$$

$$\frac{d\phi}{dt^*} = \cos^2\phi - \frac{B(\xi, \lambda)}{2}\cos 2\phi \quad (2)$$

where s is the dimensionless distance between the sphere centers [$s = r/\bar{a}$, $\bar{a} = (a_1 + a_2)/2$], λ is the size ratio of the two particles, ξ is the dimensionless separation distance between the particles ($s = \xi - 2$), and t^* is the dimension-

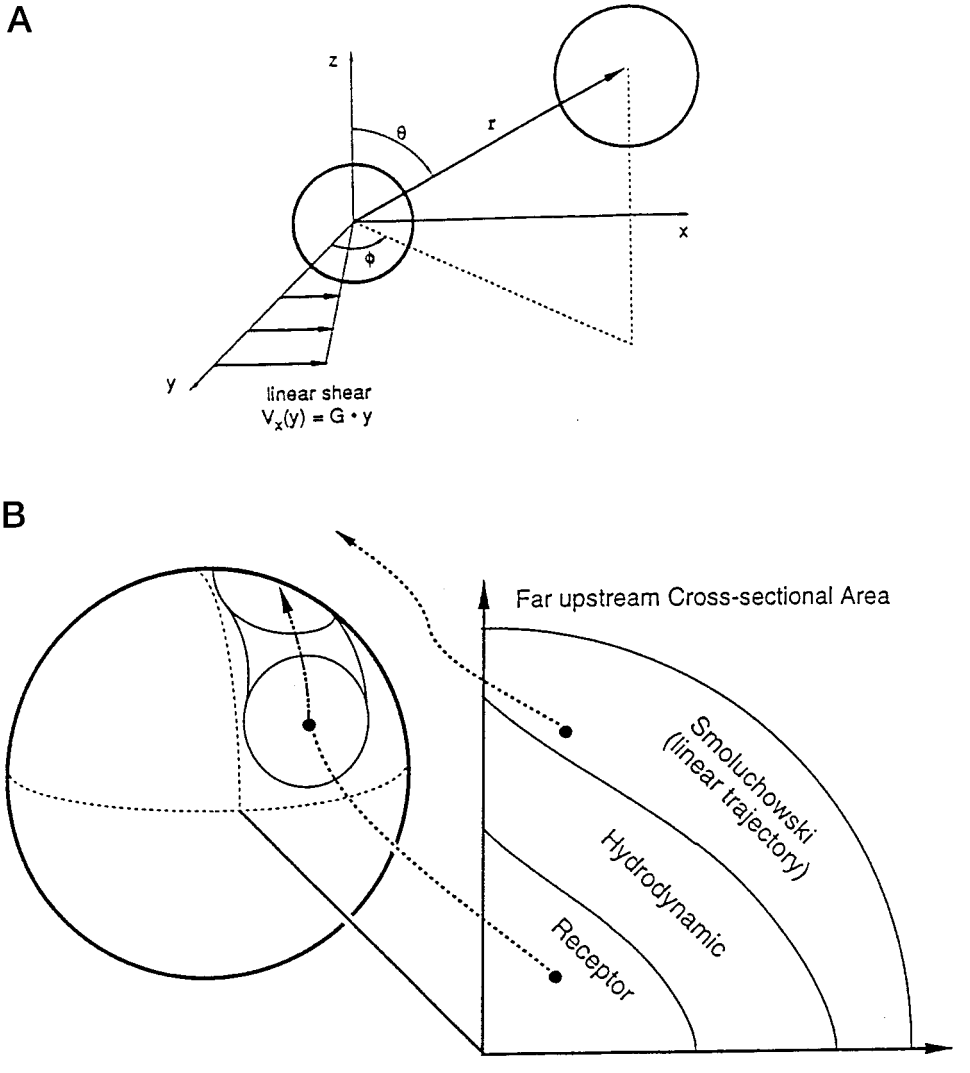

FIGURE 1 Schematic of two unequal sized neutrophils or their aggregates (of radius a_1 and a_2) in a spherical coordinate (r, θ, ϕ) system (*A*). The interaction of the particles is investigated in a linear shear field given by $V_x = Gy$, where G is the local shear rate of flow. (*B*) Schematic of different far upstream cross section. The Smoluchowski upstream area is calculated considering neutrophils following linear trajectories, and the hydrodynamic cross-section is determined from detailed hydrodynamics interactions between colliding aggregates. Whereas the particle flux through the hydrodynamic cross section represents the collision rate between aggregates of radii a_1 and a_2, the fraction of these collisions that is successful is represented by the flux through the upstream cross-sectional area labeled "receptor," which allows direct determination of ϵ_r and ϵ_{r+h}.

less time ($t^* = Gt$). In Eq. 2, F_A and F_R are the attractive and repulsion forces defined by DLVO theory, $A(\xi, \lambda)$ and $B(\xi, \lambda)$ are the mobility functions along the line of centers and normal to the line of centers of the two spheres, respectively, and $C(\xi, \lambda)$ is the correction to Stokes' law taking into account the presence of the second sphere. The mobility functions are obtained as previously described (Tandon and Diamond, 1997) for singlet-singlet ($\lambda = 1$) to singlet-sixmer interaction ($\lambda = 0.55$). The van der Waals attraction (Hamaker constant $= 10^{-19}$ J) and electrostatic repulsion ($\Psi_0 = -15$ mV) are included for completeness but have little effect on the hydrodynamics, because the particles are so rough. Equation 2 is used to carry out trajectory calculations (back-integration) to generate the far upstream area. Only particles flowing through the cross section defined by ϵ_h in Fig. 1 *B* are capable of colliding with the target particle. The flux through this upstream area is used to calculate the collision frequency. However, not all collisions result in successful binding of the colliding aggregates. Only those collisions that provide sufficient time to form enough receptor-mediated bonds to hold the colliding particles together can result in successful aggregation. Only particles flowing through the cross section defined by ϵ_r in Fig. 1 *B* are capable of forming stable aggregates during the primary collision. For two particles brought together by shear flow with collision at (θ', ϕ') on the target characterized by characteristic time of collision, $\tau(\theta', \phi')$, and swept collision area, $A_{coll}(\theta', \phi')$, a successful binding event takes place if

$$\left\{\int_0^{\tau} A_{coll}\frac{dN_b}{dt}\,dt\right\} \geq N_{crit} \qquad \text{where } N_{crit} = \frac{F_{drag}}{f_c} \tag{3}$$

f_c is the characteristic force needed to break a bond, F_{drag} [$F_{drag} = 6\pi\mu a_1 V_{eff}(1 + \lambda)$] is the drag force, and $V_{eff}(\theta', \phi')$ is the relative velocity at the instant of collision at θ', ϕ'. The very rapid bond loading rates of 5–150 pN/ms at $G = 100$–3000 s^{-1} help justify the simplified but useful model of bond breakage characterized by a single parameter, f_c (see Appendix I). The swept collision area, A_{coll}, is calculated by considering that there is an initial contact area (A_0) between the aggregates at the instant of contact at θ', ϕ' (defined by particle roughness overlap), which increases modestly as the approaching particle progresses around the target to a position of $\theta = 0$ while a growing contact area A_{coll} for bond formation is swept out (Fig. 1 *B*). At $\theta = 0$ the doublet experiences maximum shear and must satisfy the force criterion in Eq. 3 to reside within ϵ_r. The value of A_0 is 16.11 μm^2 based on 400-nm roughness, whereas Goldsmith et al. (1981) have imaged the contact in a rotating neutrophil doublet at low shear of 7.5 s^{-1} to have a diameter of 4.2 μm and an area of 14 μm^2. For a nearly head-on collision the value of A_{coll} grows to 29.3 μm^2 at $\theta = 0$. Collision time, τ, is the time needed to sweep the collision area and is estimated by calculating the characteristic distance and velocity along the direction of approach of particles for each collision at θ', ϕ' on the target surface. The geometrical considerations used to calculate A_{coll} and τ have been discussed by Tandon and Diamond (1997) (see Appendix II). As described by Tandon and Diamond (1997), the concept of the swept area allows the contact area to grow during the collision because of the cells' deformation (smearing/sweeping) over each other from the instant of contact (at θ', ϕ') to $\theta = 0$, when the "swept" contact area between the doublet is exposed to maximum shearing stresses extremely rapidly. In reality, there are compressive forces on the doublet due to normal forces as the doublet rotates during the collision. This compression would increase the contact area, especially for nearly head-on collisions and less so for glancing collisions—this dependence is captured to a first approximation in the calculation of A_{coll}.

The rate of formation of receptor-mediated bonds per unit area is calculated using the formalism of Bell (1979):

$$\frac{dN_b}{dt} = 2k_f(N_{rec,i})(N_{rec,j}) - k_r N_b \tag{4}$$

where k_f and k_r are the forward and reverse rate constants for the bond formation, and $N_{rec,i}$ and $N_{rec,j}$ are the number of active receptors *i* and *j* per unit area on the opposing colliding aggregate surfaces. For integrin-mediated binding, the reverse rate constant is considered to be very slow ($t_{1/2} > 10$ s) and is taken to be zero, whereas k_r for L-selectin-mediated binding is calculated based on the half-life of 10 ms (see Results), consistent with high-speed imaging of a 14-ms pause time of neutrophil rolling on PSGL-1 (Smith et al., 1997). Following Bell's formalism (1981), the rate constant k_f is estimated from the diffusion limit rate of association of receptors in two dimensions as

$$k_f = \eta \cdot [2\pi(D_i + D_j)] \qquad (D_i = D_j) \tag{5}$$

where η is the effectiveness factor and D_i and D_j are the diffusion constant of receptors on the opposing membranes. A value of k_f (and thus η) is determined by matching the value ϵ_{r+h} with the experimentally determined value of the overall efficiency relative to the Smoluchowski frequency.

Integrin-mediated aggregation

In the absence of L-selectin, the neutrophil aggregation at low *G* can be mediated by LFA-1 binding ICAM-3 and Mac-1 binding a putative ICAM-3-like receptor whose number and strength are identical to those of ICAM-3. Up-regulation of β_2-integrins has been modeled considering that Mac-1 and LFA receptors are in the ratio 4:15, with their total numbers per neutrophil increasing linearly from 1583/cell (8.33% of maximally active) at 0 s to 6333/cell (33.33% of maximally active) at 25 s and increasing linearly again to 10,856/cell (57% of maximally active) at 100 s, in accordance with the flow cytometer data of Taylor et al. (1996) for 1 μM fMLP stimulation of neutrophils at $t = 0$ s. The 100% maximum activity of LFA-1 and Mac-1 was taken as 10% of the maximum antigenic level (150,000

Mac-1/neutrophil; 40,000 LFA-1/neutrophil) (Diamond and Springer, 1993). The number of ICAM-3 receptors was considered to remain constant at 50,000/neutrophil at the early times before disaggregation begins after ~100 s. The rate of bond formation per unit area for integrin mediated aggregation is given as

$$\frac{dN_b^{intg}}{dt} = 2k_f^{intg}(N_{LFA-1}(t))(N_{ICAM-3}) + 2k_f^{intg}(N_{Mac-1}(t))(N_{\text{“ICAM-3”}})$$

$$k_f^{intg} = \eta_{intg} \cdot [2\pi(D_i + D_j)] \quad (6)$$

Aggregation mediated by selectin and integrins simultaneously

Neutrophil aggregation mediated by L-selectin binding with PSGL-1 in conjunction with integrins has been modeled considering 50,000 L-selectin and 10,000 PSGL-1 dimer receptors per neutrophil, using the data of Moore et al. (1991) as an upper estimate of PSGL-1 (20,000 per cell) and dividing by a factor of 2 for the role of P-selectin multimers in the measurement. The rate of formation of selectin bonds per unit area is given as

$$\frac{dN_b^{sel}}{dt} = 2k_f^{sel}(N_{L-Selectin})(N_{PGSL-1}) - k_r^{sel}(N_b^{sel})$$

$$k_f^{sel} = \eta_{sel} \cdot [2\pi(D_i + D_j)]; \quad k_r^{sel} = \ln 2/t_{1/2} \quad (7)$$

For this case of binding through multiple receptors, the total drag force is distributed among the bonds as

$$F_{drag}^{intg} = \frac{N_b^{intg}}{N_b^{intg} + N_b^{sel}} F_{drag} \quad \text{and} \quad F_{drag}^{sel} = \frac{N_b^{sel}}{N_b^{intg} + N_b^{sel}} F_{drag} \quad (8)$$

and the critical number of bonds needed to hold the colliding aggregates by selectin and integrins is calculated as

$$N_{crit}^{intg} = \frac{F_{drag}^{intg}}{f_c^{intg}} \quad \text{and} \quad N_{crit}^{sel} = \frac{F_{drag}^{sel}}{f_c^{sel}} \quad (9)$$

Two aggregates brought together by the shearing flow are held together if

$$\frac{\int_0^\tau A_{coll}(dN_b^{intg}/dt)\, dt}{N_{crit}^{intg}} + \frac{\int_0^\tau A_{coll}(dN_b^{sel}/dt)\, dt}{N_{crit}^{sel}} \geq 1 \quad (10)$$

However, if the above criterion is not strictly satisfied during the duration τ of the primary collision, any doublet with at least a single L-selectin–PSGL-1 bond is allowed to rotate as a metastable aggregate under the action of the shear flow. This is equivalent to introducing an ensemble-averaged contribution of L-selectin stochastic behavior needed to model the experimental data (see Results and Discussion). The rotation of the aggregates provides extra interaction time T_i for bonding to hold the colliding particles together, i.e., integrals on the LHS of Eq. 10 are carried over longer interaction times T_i, such that

$$T_i = \tau + n_r \tau_{rot} \quad (11)$$

where n_r is the number of rotations and τ_{rot} is the average time of rotation, given by

$$\tau_{rot} = \frac{5\pi}{6G} \quad (12)$$

We calculate the functional behavior of $n_r(G)$ and $T_i(G)$ by matching the calculated collision efficiencies with the ones observed for neutrophil aggregation in a cone-and-plate viscometer (Taylor et al., 1996).

The efficiencies reported by Taylor et al. (1996), along with their Smoluchowski-type expression (Eq. A1 in Taylor et al., 1996, $\beta_G = (16G/3)[r_i + r_j]^3$), do not match the reported “% Aggregation” data when used with the population balance equation. However, these reported efficiencies were consistent with a different expression used by Neelamegham et al. (1997), where the Smoluchowski premultiplier parameter had been taken to be 2/3 (Eq. 5 of Neelamegham et al., 1997) instead of 16/3. For our definition of shear-induced collision of spheres following linear trajectories without any hydrodynamic interaction, we use the expression in Eq. 1 that is universally identified as the Smoluchowski collision rate (Manley and Mason, 1952; Swift and Friedlander, 1964; Chang and Robertson, 1976; Friedlander, 1977; Bell et al., 1989a; Williams and Loyalka, 1991; Huang and Hellums, 1993a; Tandon and Diamond, 1997), i.e., Eq. 1 in terms of particle radii as $\beta_G = (4G/3)[r_i + r_j]^3$. Based on this relation, using methods discussed above, we matched the predicted efficiencies to the corrected measured collision efficiencies, which are one-half the values reported in figure 5c of Taylor et al. (1996). The reported values of the efficiency in Taylor et al. (1996) can be obtained using the nonstandard premultiplier of 16/3 and using the diameter of the neutrophil as its radius. To match the time-averaged efficiencies of experiment, the average collision efficiency, $\bar{\epsilon}$, over the first 30 s is calculated by integrating the overall collision efficiency $\epsilon_{r+h}(\lambda, t)$ over $t = 0$–30 s and $\lambda = 0.55$–1.

RESULTS

Selectin- and integrin-mediated cell interactions are largely studied by observations of neutrophils skipping, rolling, and arresting on endothelium or defined surfaces (Lawrence and Springer, 1991). The rheological dynamics of the contact area in neutrophil aggregation in shear flow may be somewhat different from those found in rolling adhesion experiments. We have explored neutrophil homoaggregation mediated by β_2-integrins and L-selectin accounting for two-body collision hydrodynamics, multiple receptor interactions, and time-dependent stoichiometries of the receptors. Neutrophil aggregation data were analyzed for the

shear rates of 100 s^{-1} to 3000 s^{-1} for the set of parameters in Table 1.

Integrin-mediated aggregation

In Fig. 2, we show one quadrant of the far upstream cross sections for the case of neutrophil aggregation mediated by integrins (LFA binding ICAM-3 and Mac-1 binding a putative ICAM-3-like receptor) at $G = 100\ s^{-1}$. If two neutrophils of radius a_1 and a_2 follow linear trajectories without any hydrodynamic interactions (Smoluchowski collision theory), the far upstream area (marked as β_G in Fig. 2) is a circle of radius $(a_1 + a_2)$. However, when hydrodynamic interactions between the colliding aggregates are included, only particles flowing through the cross section marked as ϵ_h are capable of coming into contact with the target particle, whereas the others actually flow around the target without collision because of hydrodynamic interactions. Smoluchowski theory overpredicts the collision frequency and is corrected by the hydrodynamic efficiency, ϵ_h (defined as the expected collision rate including hydrodynamic effects normalized with Smoluchowski collision rate). At $G = 100\ s^{-1}$ and a neutrophil concentration of 10^6/ml, the initial collision kernel ($\epsilon_h\beta_G$) with hydrodynamic interaction is 41,119 $(\mu m)^3/s$ for singlet-singlet interaction ($\epsilon_h = 0.731$). For 10^6 neutrophils/ml, the initial collision rate at $G = 100\ s^{-1}$ based on $\epsilon_h\beta_G$ is 20,560 collisions/ml/s. Thus aggregation data from experiments contain a wealth of data averaged over more than 100,000 collisions, thus justifying the ensemble-averaged kinetic formalisms of Eq. 4. To calculate these efficiencies, the neutrophil surface roughness was set at 400 nm (length of the neutrophil microvilli), the distance within which the aggregates must approach each other for a collision to take place (or the jump-off from the particle surface for starting the back-integration of the trajectory equations). In Fig. 2, only the particles flowing through the successful collision area (ϵ_r) are the ones that hit the target at an appropriate θ', ϕ' and have enough time to form enough β_2-integrin bonds ($k_f = 1.57 \times 10^{-12}$ cm^2/s or $\eta_{intg}^{LFA1} = \eta_{intg}^{Mac1} = 0.00125$ for $D_i = D_j = 10^{-10}$ cm^2/s) for successful aggregation. The flux through this cross section is used to calculate the overall efficiency of aggregation, ϵ_{r+h}, relative to the Smoluchowski frequency β_G.

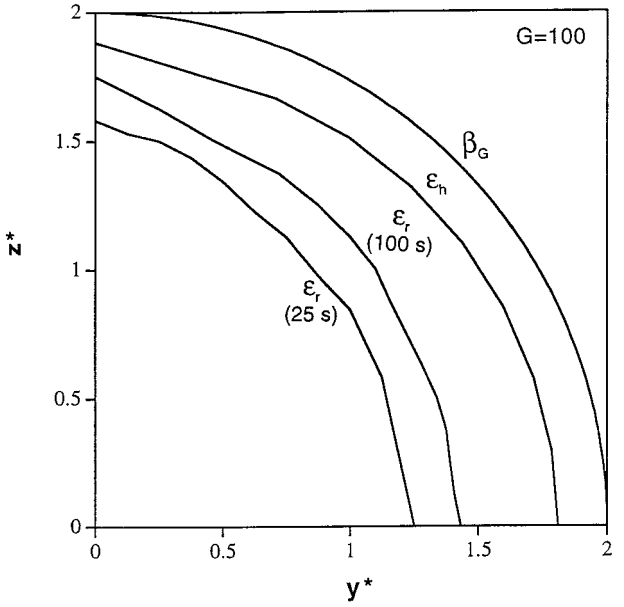

FIGURE 2 Smoluchowski (β_G), hydrodynamic (ϵ_h), and successful receptor aggregation (ϵ_r) far upstream cross section for neutrophil singlet-singlet collisions mediated by 10,855 integrins/cell (LFA-1, 2285/cell; Mac-1, 8570/cell) at 100 s post-fMLP activation without L-selectin at a shear rate of $G = 100\ s^{-1}$ and viscosity of 0.75 cP. The Smoluchowski upstream area is calculated considering neutrophils following linear trajectories, and the hydrodynamic collision area is determined from detailed hydrodynamics interactions between colliding aggregates. Whereas the particle flux through the hydrodynamic cross section represents the collision rate between aggregates of radii a_1 and a_2, the fraction of these collisions that is successful is represented by the particle flux through the ϵ_r upstream cross-sectional area. For calculating the cross-sectional area for successful aggregation, the effectiveness factor of β_2-integrin interaction was taken to be $\eta_{LFA\text{-}ICAM3} = \eta_{MAC1\text{-}"ICAM3"} = 0.00125$. For comparison, the receptor cross section for integrin-mediated aggregation is shown for neutrophils at 25 s post-fMLP activation when only 6333 active integrins (LFA-1 + Mac-1) per cell are present.

TABLE 1 Parameters for neutrophil aggregation

Parameter	Value	Reference
Neutrophil concentration	10^6/ml	Taylor et al. (1996)
Neutrophil radius	3.75 μm	Neelamegham et al. (1997) Hammer and Apte (1992)
Neutrophil surface area	176.71 μm^2	$4\pi r^2$
Neutrophil volume	220.89 μm^3	$4\pi r^3/3$
β_2-integrin bond strength	5 μdynes	Bell (1981), Lauffenburger and Linderman (1993)
Diffusion constant of receptors	10^{-10} cm^2/s	Bell (1979)
Mac-1 per neutrophil	150,000	Diamond and Springer (1993)
LFA-1 per neutrophil	40,000	Taylor et al. (1996), Granger and Schmid-Schonbein (1993)
ICAM-3 per neutrophil	50,000	Granger and Schmid-Schonbein (1993)
PGSL-1 per neutrophil	10,000	Moore et al. (1991)
L-selectin per neutrophil	50,000	Taylor et al. (1996)

The overall efficiency for integrin-mediated neutrophil aggregation at low shear rates between 100 and 400 s^{-1} as a function of time because of up-regulation of Mac-1 and LFA receptor numbers for singlet-singlet ($\lambda = 1$) and singlet-sixmer interactions ($\lambda = 0.55$) are shown in Fig. 3 *A*. To calculate these efficiencies, a single value for the β_2-integrin effectiveness factors $k_f = 1.57 \times 10^{-12}$ cm^2/s ($\eta_{intg}^{LFA1} = \eta_{intg}^{Mac1} = 0.00125$ for $D_i = D_j = 10^{-10}$ cm^2/s) was used over the range of shear rates such that the predicted time-averaged overall efficiencies were in good agreement with the (corrected) observed efficiencies of neutrophil aggregation (Taylor et al., 1996) (Fig. 3 *B*). Interestingly, this

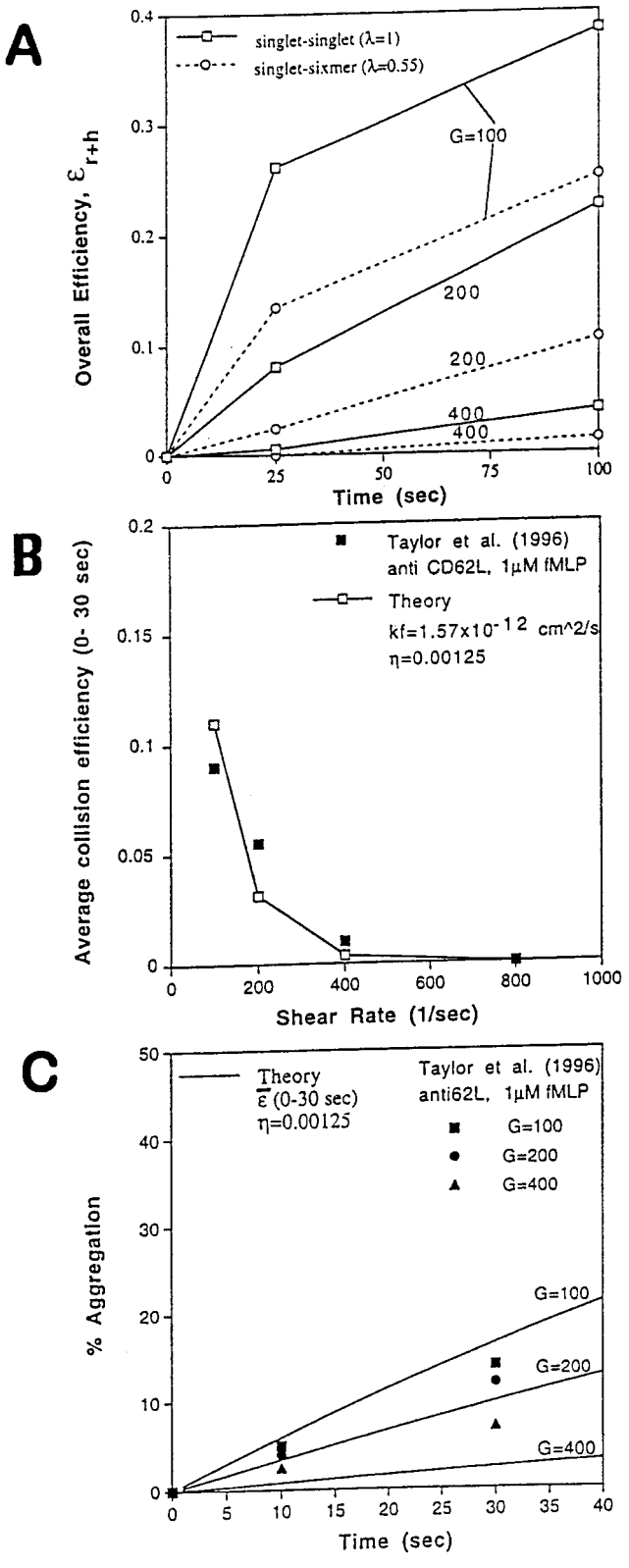

FIGURE 3 The evolution of successful collision efficiency (ϵ_{r+h}) as a function of time (in accordance with the up-regulation of integrin receptor numbers with time) for the first 100 s for integrin (LFA-1 + Mac-1)-mediated neutrophil aggregation at different shear rates is shown in *A* for singlet-singlet ($\lambda = 1$) and singlet-sixmer ($\lambda = 0.55$) collisions. The value of the effectiveness factor of integrin–ICAM3 interaction was taken to be $\eta_{\text{LFA-ICAM3}} = \eta_{\text{MAC1-ICAM3}} = 0.00125$. For this value of $\eta_{\text{intg}} = 0.00125$, the apparent integrin rate constant k_f was calculated to be 1.57×10^{-12} cm^2/s. Successful collision efficiency averaged over the first 30 s and size ratio parameter, λ, for integrin-mediated aggregation is shown in *B*. Also shown in the figures are the collision efficiencies for integrin-mediated neutrophil aggregation observed in the experiments of Taylor et al. (1996). In *C*, the calculated overall successful efficiencies (ϵ_{r+h}) are used in a population balance to predict the evolution of number densities of neutrophil aggregates of different sizes. These have been used to calculate the "% Aggregation Function" and are reported for different shear rates along with the observed evolution of "% Aggregation Function" for integrin-mediated neutrophil aggregation in the experiments of Taylor et al. (1996).

forward rate constant is in agreement with the estimate of 10^{-12} cm^2/s of Shao and Hochmuth (1997) for neutrophil CD18 binding to an anti-CD18-coated bead controlled by micromanipulation. With $k_f = 1.57 \times 10^{-12}$ cm^2/s as an estimate of the rate processes of the integrins at low shear rate of 100 s^{-1}, where L-selectin has little role in facilitating aggregation, it is possible to explore the utility of this kinetic parameter in describing aggregation at higher shear rates under conditions when L-selectin is antagonized with anti-L-selectin antibody. Consistent with the role of primary collisions (thus excluding secondary orbits or rotation of metastable doublets) as the dominant interaction mechanism for integrin mediated aggregation, $k_f = 1.57 \times 10^{-12}$ cm^2/s ($\eta_{\text{intg}} = 0.00125$) predicted the nearly hundredfold decrease in the measured, time-averaged collision efficiency as the shear rate increased from $G = 100$ to $G = 800$ s^{-1} (Fig. 3 *B*). The calculated time-averaged overall efficiencies $\bar{\epsilon}$ were used with the population balance equation (Eq. 1) to predict the evolution of aggregate number densities of different sizes. The calculated number densities as a function of time were then used to calculate the "% Aggregation Function," defined as (Taylor et al., 1996)

$$\%\ \text{Aggregation} = \left(1 - \frac{S}{S + 2D + 3T + 4Q + 5P + 6Sx^{+}}\right) \tag{13}$$

where the neutrophil aggregate number densities are given by S = singlets, D = doublets, T = triplets, Q = quartets, P = pentuplets, and Sx^{+} = sextuplets and larger aggregates. The calculated evolution of "% Aggregation Function" is shown in Fig. 3 *C* for shear rates of 100, 200, and 400 s^{-1}. Also shown in the plot is the observed "% Aggregation" at different times in the neutrophil aggregation experiments of Taylor et al. (1996). The predictions and experiments are seen to be in good agreement within a few percent of aggregation at 10 and 30 s.

An additional and independent method for estimating the value of η_{intg} is to apply the condition of colloidal stability for unstimulated neutrophils that have a low but finite number of active β_2-integrins. In this approach (Tandon and Diamond, 1997), the head-on collision at $\theta' = \phi' = \pi/2$ at the stagnation point on the back side of the target particle due to the collapsing orbit of a secondary collision will have

the maximum time for bond formation and is assigned a value of $k_{f\text{-}max}$ such that the criterion in Eq. 10 is just satisfied. All collisions except perfect head-on collisions achieved by secondary collision fail to provide successful aggregation. In Table 2, we report the values $k_{f\text{-}max}$ for which the population of unactivated neutrophils will be just stable for different values of active receptor concentrations (from 20 to 400 active LFA-1 and 75 to 1500 active Mac-1/neutrophil) on the unstimulated neutrophil surface at a shear rate of 50 s^{-1}. We found that the estimated values of $k_{f\text{-}max}$ for colloidal stability are in the same range as the value of k_f determined to predict the aggregation data of Taylor et al. (1996) in Fig. 3 *B*. At $G = 50\ s^{-1}$, neutrophils with up to ~600 active β_2-integrin receptors will fail to aggregate for $k_f = 1.57 \times 10^{-12}$ cm^2/s. Once more than ~4% of the maximum concentrations of active Mac-1 and LFA-1 are exposed, corresponding to only 0.4% of the total CD11a and CD11b antigen levels, the cells are predicted to aggregate, albeit slowly.

L-Selectin-mediated interactions

Neutrophil aggregation mediated simultaneously by β_2-integrins and L-selectin displays extremely complex behaviors. Facilitation of neutrophil aggregation by L-selectin involves its binding to PSGL-1 dimer receptors on the surface of the opposing neutrophil. There are ~50,000 L-selectin and ~10,000 PSGL-1 receptors per neutrophil. L-selectin alone is not sufficient to mediate aggregation. However, in the presence of β_2-integrins, L-selectin causes a marked enhancement of aggregation (Taylor et al., 1996), especially at $G \geq 400\ s^{-1}$. The rapid formation of short-lived L-selectin bonds is considered to facilitate the slower but more stable integrin bonding as aggregation proceeds in a shear field. Metastable aggregates held together by L-selectin likely rotate in the shear field and have more time for formation of the integrin bonds needed to hold the aggregates together in a stable manner. We do not consider disaggregation processes due to receptor shedding or down-regulation in the first 30 s.

To estimate the parameters (k_f^{sel}, k_r^{sel}, f_c^{sel}) needed to model L-selectin–PSGL-1 binding, we calculated the overall efficiency, ϵ_{r+h}, for singlet-singlet interaction ($\lambda = 1$) mediated by L-selectin alone at $G = 100\ s^{-1}$, for various combinations of these parameters (Table 3). It is known that L-selectin does not mediate appreciable aggregation by itself. The half-life of the L-selectin–PSGL-1 bond has recently been reported to be ~10–15 ms (Smith et al., 1997) as measured by high-speed imaging of rolling neutrophils on PSGL-1, although longer half-lives of ~150 ms are observed if imaged at video rates (Alon et al., 1997). For the half-life of L-selectin–PGSL of 10 ms and k_f^{sel} equal to k_f^{intg}, a value of f_c^{sel} of 1 μdyne resulted in essentially no aggregation ($\epsilon < 0.001$), consistent with experimental observations of colloidal stability of resting isolated neutrophils. We have used these values to model selectin-mediated neutrophil aggregation. Values of $k_f^{sel} < k_f^{intg}$ are less likely (but not impossible), given the kinetic advantage of microvilli presentation of L-selectin. Interestingly, Shao and Hochmuth (1997) reported that neutrophil L-selectin and CD18 bind to anti-L-selectin and anti-CD18 on beads, respectively, at similar on rates. At values of $k_f^{sel} = 1.57 \times 10^{-12}$ cm^2/s and $f_c^{sel} = 1$ μdyne, half-lives of 100 ms and 1000 ms will result in appreciable aggregation ($\epsilon > 0.001$) of resting neutrophils. Similarly, if the selectin forward rate constant is 5 or 10 times faster than that of k_f^{intg}, for nonappreciable aggregation of resting neutrophils, the selectin bond strength would need to be on the order of 0.1 μdynes (1 pN), a value too small to be likely (for short durations under stress) based on the micromanipulation data and rolling adhesion data that are available for the L-selectin bond strength.

TABLE 2 Value of effectiveness factor, η_{intg}, at which the neutrophil populations are just stable for increasing numbers of LFA-1 + Mac-1 receptors on the neutrophil surface

% of maximally active LFA-1 plus Mac-1	η_{max}	$k_{f\text{-}max} \times 10^{12}$ (cm^2/s)
0.5	0.006	7.54
1	0.003	3.77
2	0.001	1.26
3 nonaggregating	0.001	1.26
4 aggregating	0.0007	0.88
5	0.0006	0.75
6	0.0005	0.63
7	0.0004	0.50
8	0.0003	0.38
9	0.0003	0.38
10	0.0003	0.38

The total number of maximally active Mac-1 and LFA-1 are 19,000/neutrophil, corresponding to 10% of the total surface antigen concentration for LFA-1 and Mac-1 (40,000 LFA-1 and 150,000 Mac-1). At $G = 50\ s^{-1}$, neutrophils with up to ~600 active β_2-integrin receptors will fail to aggregate for $\eta_{intg} = 0.00125$.

L-selectin- and β_2-integrin-mediated aggregation

In Fig. 4, we show the far upstream cross section for primary collisions for aggregation mediated by integrins and L-selectin simultaneously at $G = 400\ s^{-1}$. The overall efficiency, ϵ_{r+h}, corresponding to the ϵ_r primary collision cross section relative to β_G substantially underpredicts the observed efficiencies of Taylor et al. (1996). Also shown in Fig. 4 is the upstream cross section for all primary collisions that result in at least one L-selectin bond, the flux through which would substantially overestimate the measured efficiency. This is seen in Fig. 5 *A* for the efficiency for primary collisions ($n_r = 0$) and for the efficiency for all primary collisions with at least one L-selectin bond ($n_r = \infty$). In our calculations, we estimate the average rotation number of metastable aggregates needed for a given shear rate to match the collision efficiencies of neutrophil aggregation observed in the experiments of Taylor et al. (1996). In Fig. 5

TABLE 3 Sensitivity of the overall efficiency (ϵ_{r+h}) to different parameters for the L-selectin–PSGL-1 bond (k_f^{sel}, k_r^{sel}, f_c^{sel})

		Efficiency ($\lambda = 1$)		
$k_f^{L\text{-}sel}$	f_c (μdynes)	$t_{1/2} = 10$ ms	$t_{1/2} = 100$ ms	$t_{1/2} = 1000$ ms
$1 \times k_f^{intg}$	0.1	<0.001	<0.001	<0.001
	0.5	<0.001	0.0136	0.0202
	1.0	<0.001	0.0942	0.105
	5.0	0.142	0.346	0.381
$5 \times k_f^{intg}$	0.1	<0.001	0.0136	0.0202
	0.5	0.130	0.27	0.29
	1.0	0.290	0.414	0.414
	5.0	0.563	0.594	0.609
$10 \times k_f^{intg}$	0.1	0.006	0.094	0.105
	0.5	0.290	0.414	0.414
	1.0	0.449	0.510	0.510
	5.0	0.646	0.650	0.650

$k_f^{intg} = 1.57 \times 10^{12}$ cm^2/s ($\eta_{intg} = 0.00125$).

The fact that resting neutrophils do not aggregate in a shear field requires $\epsilon_{r+h} < 0.001$ as a condition of colloidal stability. The combination of $k_f^{sel} = 1.57 \times 10^{-12}$ cm^2/s, $f_c^{sel} = 1$ μdyne, and $t_{1/2} = 10$ ms was seen to be consistent with the experimental observation of no aggregation of resting neutrophils. This set was used to model neutrophil aggregation with contributions by L-selectins.

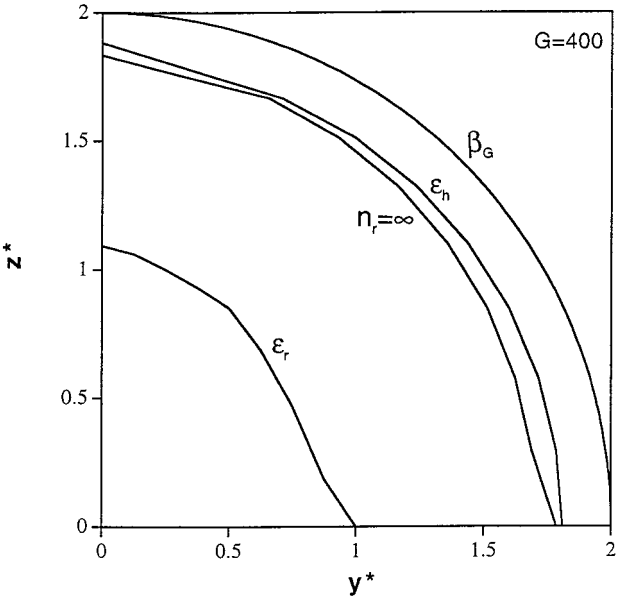

FIGURE 4 Smoluchowski (β_G), hydrodynamic (ϵ_h), and successful receptor upstream (ϵ_r) cross-sectional area for the case of neutrophil aggregation mediated by selectin and integrin simultaneously is shown for $G = 400$ s^{-1}. Only particles flowing through the area denoted ϵ_r provide sufficient time to form enough bonds during primary collision to hold the colliding neutrophils together. Also shown in the figure is the cross section for all collisions that result in at least one L-selectin bond (ϵ_r, $n_r = \infty$).

A, we present the time-averaged overall collision efficiency ϵ_{r+h} for different average rotation numbers n_r in the shear rate range between 100 and 3000 s^{-1} and at a buffer viscosity of 0.75 cP. Also shown in the plot are the corrected collision efficiencies observed in the experiments of Taylor et al. (1996). Whereas at the lowest shear rates (100 s^{-1} and 200 s^{-1}) the observed efficiencies could be matched by primary collision phenomena that result in shear stable aggregates, longer interaction times requiring doublet rotation are needed to explain the observed efficiencies for shear rates of 400 s^{-1} and above. The number of rotations is calculated to increase from 8 to 50 as the shear rate increases from 400 to 3000 s^{-1}. The corresponding efficiencies for different rotation numbers $n_r(G)$ and at different shear rates at the higher viscosity of 1.7 cP are shown in Fig. 5 B. Based on Fig. 5, A and B, average roll numbers, $n_r(G)$, were calculated as a function of shear rate such that the predicted efficiencies matched the observed collision efficiencies. The calculated average roll numbers, $n_r(G)$, and average interaction time, $T_i(G) = n_r(G) \times \tau_{rot}$, where $\tau_{rot} = 5\pi/6G$ for buffer viscosities of 0.75 cP and 1.7 cP, are plotted in Fig. 5 C. Interestingly, the number of rotations was seen to be largely insensitive to a 2.27-fold increase in buffer viscosity and a consequent increase in the drag force on the aggregates. The calculated interaction times were almost constant, falling in the narrow range of 44 and 65 ms (52.53 ± 8.5, $n = 8$) for shear rates between 400 s^{-1} and 3000 s^{-1} and for buffer viscosities of 0.75 cP and 1.7 cP. This interaction time may reflect a characteristic time when L-selectin bonding is essentially at equilibrium in the contact area or when integrin bonding can stabilize a firm adhesion. In our calculation of selectin-facilitated aggregation, 95.3% and 98.9% of the L-selectin–PSGL-1 bonds at equilibrium will be formed at 44 and 65 ms, respectively (Fig. 5 D). At equilibrium, we predict that only 0.025% of L-selectin is actually bound (13 bonds) in the contact area of 29.3 μm^2. The 50-ms interaction time may also represent several half-lives for a group of L-selectin bonds to decay to stochastic levels (0, 1, or 2 bonds).

With the values of $n_r(G)$ and interaction time $T_i = n_r(G) \times \tau_{rot}$ that predict the measured collision efficiencies of activated neutrophils through L-selectin, LFA-1, and Mac-1 interactions (Fig. 5 C), it is possible to predict the extent of aggregation that exists at a given shear rate when one of the integrins is blocked by antibody. At $G = 400$ s^{-1}, a total of eight rotations was required for the activated neutrophil to aggregate at the measured efficiency in the absence of any blocking antibodies (Fig. 5 A). When blocking antibody against LFA-1 is present (Fig. 6), the collision efficiency at 400 s^{-1} is reduced only slightly, and the percentage aggregation facilitated by L-selectin is impaired by only a few percent, both in the experiments of Taylor et al. (1996) as well as in the simulation using $n_r(G = 400\ s^{-1}) = 8$ without LFA-1. It is likely that the k_f of Mac-1 is slightly overestimated, but a more refined determination of the Mac-1 forward rate constant would be justified when the counter-receptor is known or both L-selectin and LFA-1 are antagonized in concert. When blocking antibody against Mac-1 is present, the percentage aggregation that is facilitated by L-selectin is impaired more dramatically in the experiments

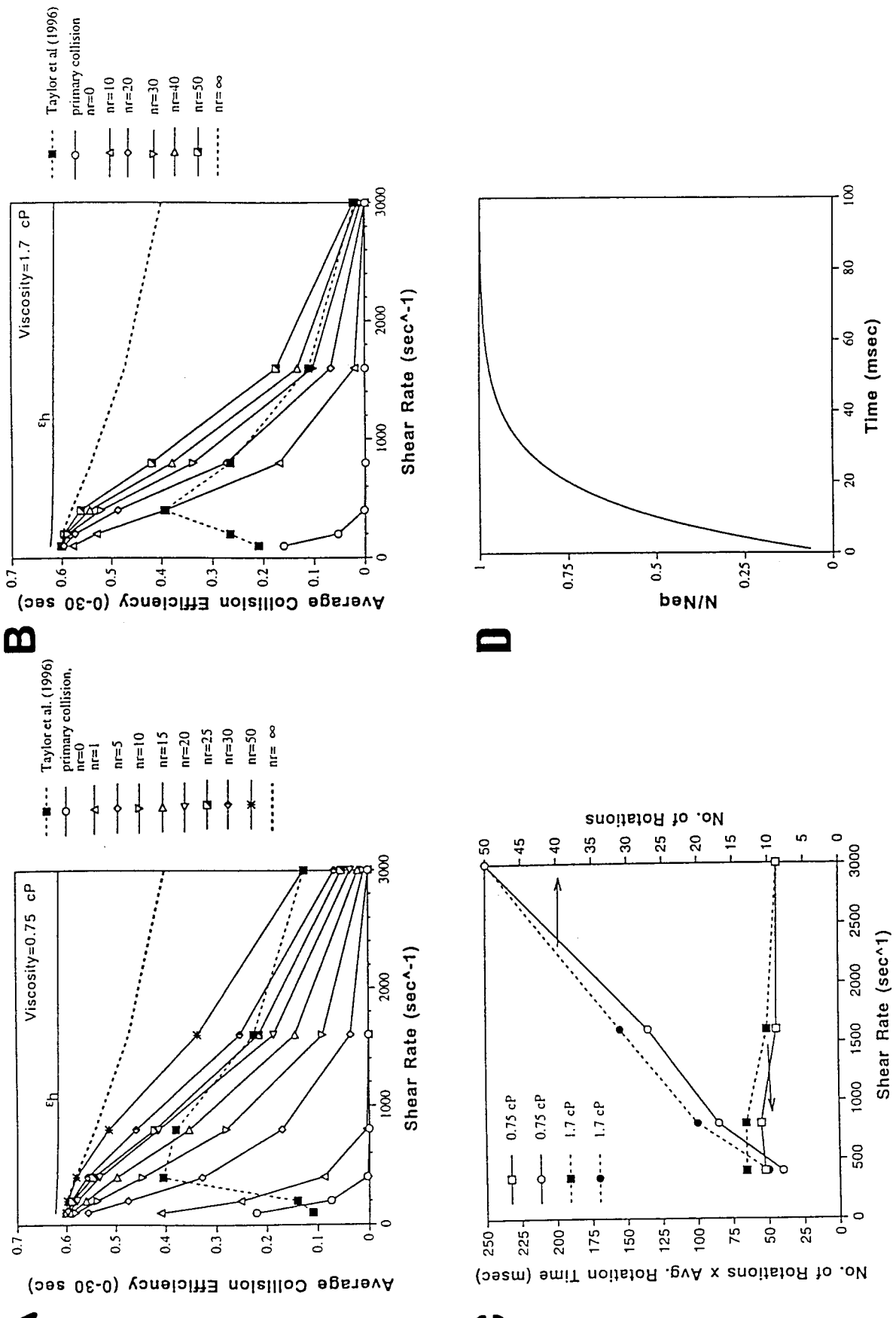
A
Average Collision Efficiency (0-30 sec)
Viscosity=0.75 cP
εh
Shear Rate (sec^-1)
Taylor et al. (1996)
primary collision, nr=0
nr=1
nr=5
nr=10
nr=15
nr=20
nr=25
nr=30
nr=50
nr= ∞
B
Average Collision Efficiency (0-30 sec)
Viscosity=1.7 cP
εh
Shear Rate (sec^-1)
Taylor et al (1996)
primary collision nr=0
nr=10
nr=20
nr=30
nr=40
nr=50
nr= ∞
C
No. of Rotations x Avg. Rotation Time (msec)
No. of Rotations
Shear Rate (sec^1)
0.75 cP
0.75 cP
1.7 cP
1.7 cP
D
N/Neq
Time (msec)

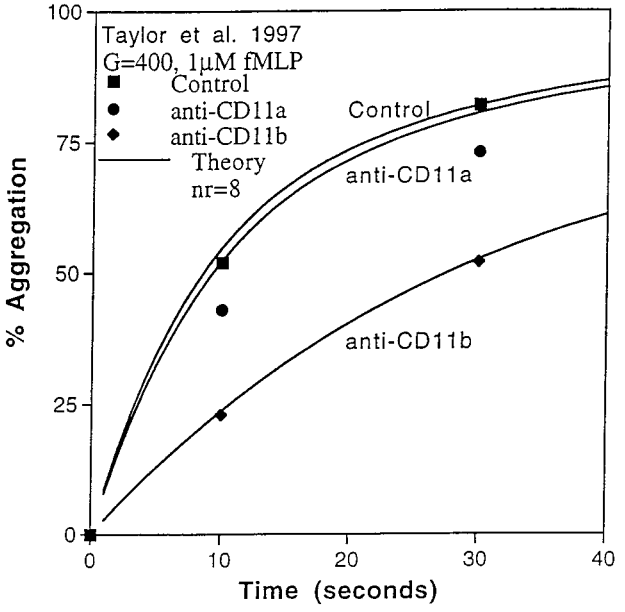

FIGURE 6 The predicted evolution of "% Aggregation" at $G = 400\ s^{-1}$ ($n_r(G) = 8$) for activated neutrophil or when LFA-1 or Mac-1 was blocked by anti-CD11a or anti-CD11b. Also shown in the figure is the observed % Aggregation in experiments of Taylor et al. (1996), for aggregation without antibody (■), with antiCD11a (●), and with antiCD11b (◆).

of Taylor et al. (1996) and in the simulation using $n_r(G = 400\ s^{-1}) = 8$ without Mac-1. Over the first 30 s of aggregation at $400\ s^{-1}$, when metastable aggregates rotate eight times on average, the model predicted aggregate formation in the presence of L-selectin with 1) both LFA-1 and Mac-1, 2) LFA-1 alone, or 3) Mac-1 alone. Even in the presence of L-selectin facilitation of doublet formation at $400\ s^{-1}$, the kinetics and strengths of the individual integrin contributions in Fig. 6 are accurately predicted on the basis of integrin properties obtained independently of L-selectin (Fig. 3 *B*).

The calculated efficiencies were used in a population balance framework to predict the evolution of number densities of aggregates of different sizes. We present the number densities for the first 35 s at $G = 800\ s^{-1}$ in Fig. 7. Our predictions were in agreement with the flow cytometry measurements of Neelamegham et al. (1997) for the first 10 s but tended to underpredict the number densities for aggregates with sizes smaller than sextuplets at times greater than 30 s. This underprediction can be explained by disaggregation of the largest aggregation bin (6+). The largest aggregates (6+) may have increased lability and sensitivity to hydrodynamic forces in the experiment that are not accounted for in the model in Eq. 1c.

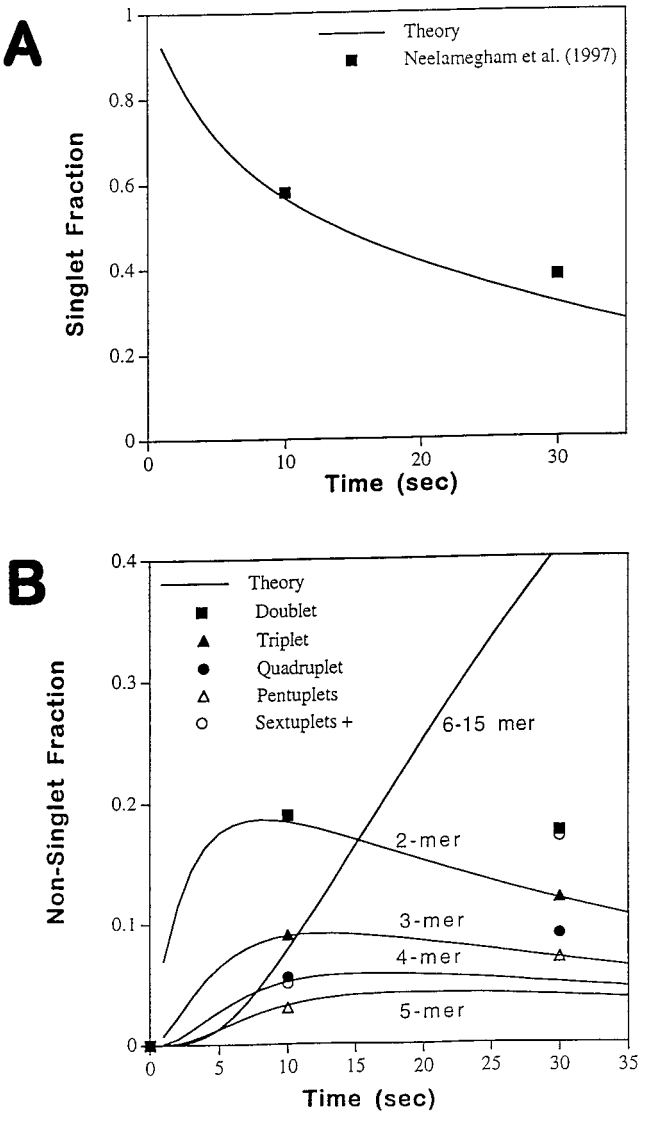

FIGURE 7 The evolution of number densities of neutrophil aggregates of different sizes for neutrophil aggregation at $800\ s^{-1}$ in the presence of L-selectin is shown along with the observed number densities in the cone and plate viscometer neutrophil aggregation data of Neelamegham et al. (1997).

L-selectin- and β_2-integrin-mediated aggregation at $G = 100\ s^{-1}$

The experimentally observed aggregation of activated neutrophils at $100\ s^{-1}$ is unusually inefficient ($\epsilon \approx 0.1$) compared to that observed at $G > 400\ s^{-1}$, where $\epsilon \approx 0.4$ (see Fig. 5, *A* and *B*) (Taylor et al., 1996). As Taylor et al. (1996) indicate, this likely involves cell deformation or enhanced

FIGURE 5 Calculated overall efficiency (ϵ_{r+h}) for activated neutrophil as a function of shear rate for primary collisions and different number of rotations (n_r) for aggregation mediated by β_2-integrins and selectin simultaneously at the fluid viscosity of 0.75 cP (*A*) or 1.7 cP (*B*). Also shown in the plots are the observed collision efficiencies (Taylor et al., 1996). In *C*, the number of rotations (*circles*) and the interaction times (*squares*) (T_i = number of rotations × rotation time) were obtained by matching the calculated efficiencies with the observed collision efficiencies at each shear rate from *A* for 0.75 cP viscosity (*open symbols*) and from *B* for 1.7 cP (*solid symbols*). The observed interaction time (~50–60 ms) corresponds to a characteristic time when L-selectin–PSGL-1 bonding is at 95% of equilibrium (*D*).

microvilli delivery to the contact area, as in Finger et al. (1996) and Lawrence et al. (1997), and is not expected on classical kinetic considerations, because bonds have the most time to form during the primary collision at $G = 100\ s^{-1}$. At higher G, the force of compression during doublet rotation is increased (see Appendix I). In Fig. 8, we present simulations of aggregation involving L-selectin, Mac-1, and LFA-1 at $G = 100\ s^{-1}$. If L-selectin can bond at the rate observed in high shear experiments of $G > 400\ s^{-1}$, then aggregation is significantly overpredicted for interaction times of ~50 ms ($n_r \approx 1$) or for aggregation mediated only by primary collision ($n_r = 0$). This can be seen in the overall efficiencies given in Fig. 5 *A* at $G = 100\ s^{-1}$, where primary collisions and one rotation both overpredict the measured value. If L-selectin bonding is neglected ($k_f^{sel} = 0$), then aggregation at $G = 100\ s^{-1}$ of activated neutrophils without blocking antibodies or with anti-LFA-1 is accurately predicted; however, aggregation with anti-Mac-1 present is underpredicted (Fig. 8). At $G = 100\ s^{-1}$, the simulations indicate that L-selectin bonding is not fully functional (Finger et al., 1996; Taylor et al., 1996; Lawrence et al., 1997) at the rate seen at $G > 400\ s^{-1}$ (Fig. 5 *C*). We predict that it may be possible to observe the attenuated contribution of L-selectin at $G = 100\ s^{-1}$ if Mac-1 is antagonized in the presence and absence of L-selectin antagonism. Without Mac-1 antagonism, the relatively small L-selectin contributions are largely masked by the sufficient Mac-1 mediation of aggregation during the primary collision at $G = 100\ s^{-1}$. The simulations indicate that above $400\ s^{-1}$, L-selectin is fully functional, and the observed maximum (Taylor et al., 1996) in efficiency in Fig. 5, *A* and *B*, is due to a shift from aggregation mediated by primary collisions (where L-selectin activity is attenuated) to aggregation mediated by L-selectin facilitation of metastable aggregates that rotate for ~50 ms at $G > 400\ s^{-1}$. The attenuation of L-selectin function at $G < 400\ s^{-1}$ corresponds to about a twofold reduction in k_f^{sel} to predict the observed LFA-1-mediated aggregation in the presence of active L-selectin, but with Mac-1 antagonism (simulation not shown).

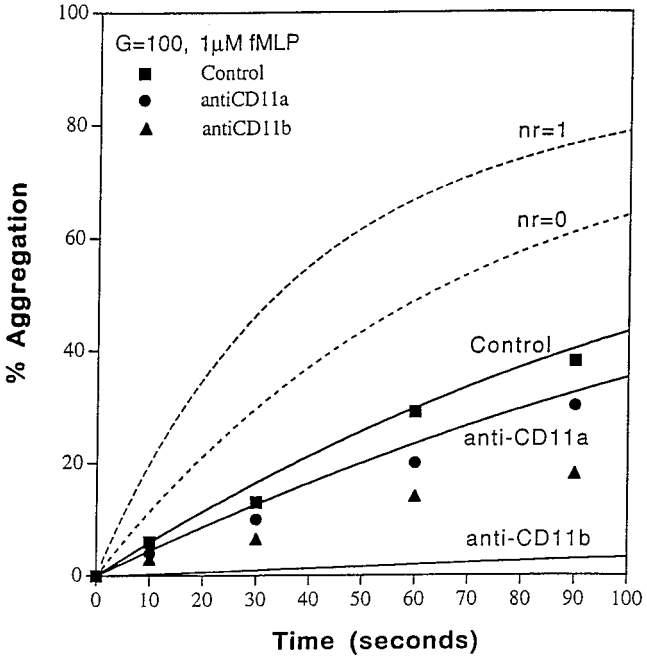

FIGURE 8 The predicted evolution (——) of "% Aggregation" in the absence of L-selectin at $G = 100\ s^{-1}$ for activated neutrophil or when LFA-1 or Mac-1 was blocked by anti-CD11a or anti-CD11b. Also shown in the figure is the observed % Aggregation in experiments of Taylor et al. (1996), for aggregation without antibody (■), with antiCD11a (●), and with antiCD11b (◆). If L-selectin can bond at the rate observed at high shear experiments of $G > 400\ s^{-1}$, then aggregation is significantly overpredicted for primary collisions ($n_r = 0$) or one rotation ($n_r = 1$, ——).

DISCUSSION

For an apparent $k_f^{intg} = 1.57 \times 10^{-12}\ cm^2/s$ ($\eta_{intg} = 0.00125$), we were able to predict the collision efficiencies of neutrophil aggregation mediated by only β_2-integrins (Mac-1 and LFA-1), which were consistent with the efficiencies observed in the experimental setup of Taylor et al. (1996) for shear rates between 100 and $800\ s^{-1}$. For the case of aggregation in the presence of L-selectin at $G > 400\ s^{-1}$, we calculate that metastable aggregates are formed that rotate for ~50 ms under the influence of the flow field, providing more time for binding. We found that the average interaction time (number of rotations × time of rotation) was between 45 and 65 ms, largely independent of the shear rate and buffer viscosity. This characteristic time may reflect a characteristic time for L-selectin–PSGL-1 bonding to equilibrate. In Table 4, we summarize the calculated kinetics and strength of a different set of receptors that predict the measured neutrophil aggregation under flow conditions. We calculate that the aggregation of neutrophils at low shear rate ($G < 400\ s^{-1}$) likely proceeds by primary collisions. As the shear rate increases, L-selectin becomes fully functional, to allow metastable aggregates to rotate for ~50 ms to become stable by β_2-integrin bonding.

Selectin bonding is stochastic and displays significant shear stress dependency, both in the probability of bond formation and in the probability of bond breakage. As a deterministic model, the three-parameter model for L-selectin function (k_r, k_f, f_c) did not simultaneously predict all four criteria imposed by experimental observation: 1) unactivated neutrophils do not aggregate in flow; 2) L-selectin alone cannot mediate aggregation of activated neutrophils; 3) L-selectin enhances homoaggregation at all shear rates; and 4) L-selectin function increases as the shear rate (or shear stress) is increased. The three parameters describing L-selectin were chosen to satisfy criteria 1 and 2, using k_r derived from direct experimental observation of Smith et al. (1997). Criterion 3 required relaxation of the force criterion (Eq. 10) at the end of the primary collision by allowing doublets that merely satisfy a kinetic criterion of the primary collision (number of L-selectin bonds > 1 from Eq. 7) to survive transiently for some longer interaction time T_i (Eq. 11). These metastable doublets must satisfy or fail to

TABLE 4 Summary of neutrophil receptor kinetics

A	*B*	# *A*(*t*)/cell*	# *B*/cell	η	k_f (cm^2/s)	k_r (s^{-1})	f_c (μdynes)	$\dot{N}_b(t)$ (#/μm^2/s)*
LFA-1	ICAM-3	333 → 2285	50000	0.00125	1.57×10^{-12}	—	5	0.083 → 0.574
Mac-1	"ICAM-3"	1250 → 8570	50000	0.00125	1.57×10^{-12}	—	5	0.311 → 2.13
L-selectin	PGSL-1	50000	10000	0.00125	1.57×10^{-12}	69.3	1	2.49

*Time-dependent values are given for t = 0^+ s to 100 s after 1 μM fMLP stimulation.

satisfy the force criterion (Eq. 10) imposed at some later interaction time T_i. This four-parameter model of selectin function corresponds to introducing the ensemble average of a stochastic process. It was remarkable to observe that a single interaction time of ~50 ms described the aggregation phenomena observed between $G = 400$ and 3000 s^{-1}. Ideally, a stochastic model, as in Chang and Hammer (1996), that satisfies the above four criteria would yield a mean doublet lifetime of 50 ms when averaged over the distribution of collisions. No attempt was made to develop a model to meet criterion 4.

With regard to criterion 4, we have found that reducing the L-selectin k_f by a factor of 2 can predict exactly the neutrophil homoaggregation at $G = 100$ s^{-1} mediated by L-selectin and LFA-1 (with anti-CD11b present). However, at $G = 100$ s^{-1}, reducing the L-selectin forward rate by half overpredicted by ~7 Percent Aggregation the Mac-1-mediated aggregation at 90 s with anti-CD11a present and overpredicted by ~9 Percent Aggregation at 90 s the aggregation in the absence of any blocking Fab. Given that we likely have slightly overestimated the k_f of the Mac-1–"ICAM-3" reaction as previously discussed in regard to Fig. 6 (also note the slight overprediction of ϵ in Fig. 3 *B* at $G =$ 100 s^{-1}), these overpredictions in Percent Aggregation at 90 s would be reduced substantially by using a slightly slower k_f for the Mac-1–"ICAM-3" reaction. With distinct values of k_f for the LFA-1 and Mac-1 reactions and a reduced k_f for L-selectin ($= k_f/2$), the model does provide quantitative prediction for aggregation at $G = 100$ s^{-1} mediated by L-selectin ± LFA-1 ± Mac-1.

We have used the concept of a characteristic force to break a bond to estimate the number of bonds needed to hold the colliding aggregates together as originally proposed by Bell (1981). In general, the number of bonds needed is a complex function of loading rates, the time over which the force is applied, and the nonuniform loading of bonds (Chang and Hammer, 1996; Dembo et al., 1988). However, when the loading rates are rapid enough (~1 pN/ms or higher), then the concept of an average characteristic force needed to break a bond appears to be useful in explaining some but not all of the average aggregation properties of platelets and neutrophils in flow. For the case of collisions between neutrophil singlets at $G = 100$ s^{-1}, forces and loading rates are calculated (Appendix I) to be on the order of 10 pN and 5 pN/ms, respectively, suggesting that the assumption of characteristic bond strength is a reasonable one. The predicted forces and loading rates scale linearly with increase in the shear rate. We made no attempt to model the time-dependent force loading of a deformable and variable-sized contact area held together by discrete reversible bonds that can diffuse in the contact area. Thus Eq. 10 contains the kinetics and mechanics of bond formation and disruption and utilizes a constant off rate for stressed bonds. Whereas integrin function is well described by Eq. 10 (see Fig. 3), L-selectin function required an additional parameter, T_i, to predict the observed phenomena.

The theoretical approach developed for platelet β_3 integrin GPIIb/IIIa gave $k_f = 1.78 \times 10^{-11}$ cm^2/s (Tandon and Diamond, 1997) when used to simulate platelet consumption data of Bell et al. (1989a,b), whereas neutrophil β_2 integrins were calculated to have $k_f = 1.57 \times 10^{-12}$ cm^2/s in the absence of L-selectin interactions. Interestingly, the calculated value of k_f for β_2 integrins is potentially underpredicted and may be closer to the calculated platelet β_3 value, because recent evidence (del Pozo et al., 1994) indicates that ICAM-3 is slowly released by neutrophils over several minutes, and its surface concentration is not kept constant at larger times, as assumed in the present calculations. Moreover, the β_3-integrin forward rate determination assumed that plasma fibrinogen was instantaneously equilibrated with active GPIIb/IIIa, which thus gives an upper estimate of k_f by reducing the amount of unbound GPIIb/IIIa available for bonding. If β_2 and β_3 integrin association rates are relatively similar in reality for neutrophils and platelets, then the model successfully deconvoluted receptor kinetics, stoichiometry, cell size, and hydrodynamics for aggregation studies conducted with very different cell types in different laboratories.

To calculate the L-selectin parameters (k_f^{sel}, k_r^{sel}, f_c^{sel}) for modeling L-selectin facilitation of aggregation, we have used parameters based on the observation that resting neutrophils that present L-selectin and PSGL-1 do not aggregate appreciably in flow. The half-life of the L-selectin–PSGL-1 bond has been recently reported to be ~14 ms (Smith et al., 1997), as measured by high-speed imaging of rolling neutrophils. This half-life is significantly smaller than the half-life of a P-selectin–PSGL-1 bond (Alon et al., 1995). For the half-life of L-selectin–PGSL of 10 ms and $k_f^{sel} = k_f^{intg}$, a value of f_c^{sel} of 1 μdyne predicted no aggregation ($\epsilon < 0.001$), consistent with experimental observations of colloidal stability of resting neutrophils. At values of $k_f^{sel} = k_f^{intg}$ and $f_c^{sel} = 1$ μdyne, half-lives of 100 ms and 1000 ms would result in appreciable aggregation. Evolutionary pressure may select against L-selectin mutations that provide for longer-lived L-selectin–PSGL-1 bonds ($t_{1/2} \geq$ 100 ms), because the aggregation of resting neutrophils is

highly disadvantageous. We have not explored the neutrophil colloidal stability criterion for $k_f^{sel} < k_f^{intg}$, because selectins are recognized to form bonds faster than integrins because of their presentation on the microvilli. Still, issues of receptor number also influence the interpretation of selectins as faster bonding molecules than integrins, especially in aggregation studies, where compression of the doublet may give excellent membrane contact.

We have developed a method to systematically predict the effects of hydrodynamics, β_2-integrin, and L-selectin bond formation and dissociation rates on the neutrophil aggregation efficiency. The method is useful for deconvoluting fundamental reaction parameters and may provide insight into neutrophil adhesion to the vessel wall under flow. Neutrophil recruitment at the site of inflammation involves neutrophil rolling on the cell surface, followed by adhesion (Lawrence and Springer, 1991). Further capture of additional flowing neutrophils by adherent neutrophils occurs via L-selectin (Bargatze et al., 1994). We are now extending these methods to develop tools for a better understanding of heterotypic aggregation between platelets (Tandon and Diamond, 1997) and neutrophils in shear flow.

APPENDIX I: CALCULATION OF FORCES AND LOADING RATES

To illustrate the forces and loading rates, we have used the formulation of Tha and Goldsmith (1986) to calculate the forces (shear, normal, and total) and loading rates for two sphere singlets acting as a doublet. The shear and normal forces have been calculated to be (Tha and Goldsmith, 1986)

$$F_{shear} = \alpha_{yz}\mu G a_1^2[(\cos 2\theta_y \cos \phi_y)^2 + (\cos \theta_y \sin \phi_y)^2]^{1/2}$$

$$F_{normal} = \alpha_x \mu G a_1^2 \sin^2 \theta_z \sin 2\phi_z \qquad \text{(A1)}$$

where α_{yz} and α_x are reported in Tha and Goldsmith (1986) and θ_i and ϕ_i are the azimuthal and radial angles with respect to the ith axis. Shear and normal forces at $G = 100\ s^{-1}$ ($\lambda = 1$), along with the loading rates, were calculated for the angle $\bar{\theta} = \tan^{-1}(2\tan(\pi/6))$ corresponding to the average rotation time and are reported in Fig. 9.

Aggregates rotating as doublets experience these complex time varying normal forces (F_{normal}) and shear forces (F_{shear}) depending on the position relative to the shear field and the plane of the rotation (Fig. 9). To incorporate this information as part of the calculations would require computationally intensive forward integration in time as the aggregate rotates with the force laws applied at every position during rotation for every combination of (θ', ϕ'). Because such calculations were not practical, we chose to use an average drag force (F_{drag}) instead for our calculations. F_{drag} is on the order of the total force acting on the aggregates and has an implicit dependence on (θ', ϕ') through $V_{eff}(\theta', \phi')$.

APPENDIX II: CALCULATION OF COLLISION TIME τ AND COLLISION AREA A_{coll}

The collision τ for a given collision initiated at θ', ϕ' on the target surface is calculated by defining a characteristic distance and velocity along the direction of approach of particles at the instant of contact. It is thus estimated to be

$$\tau = \frac{a_1(1 + \lambda)\sin \theta' \sin \phi'}{v_x} \qquad \text{(A2)}$$

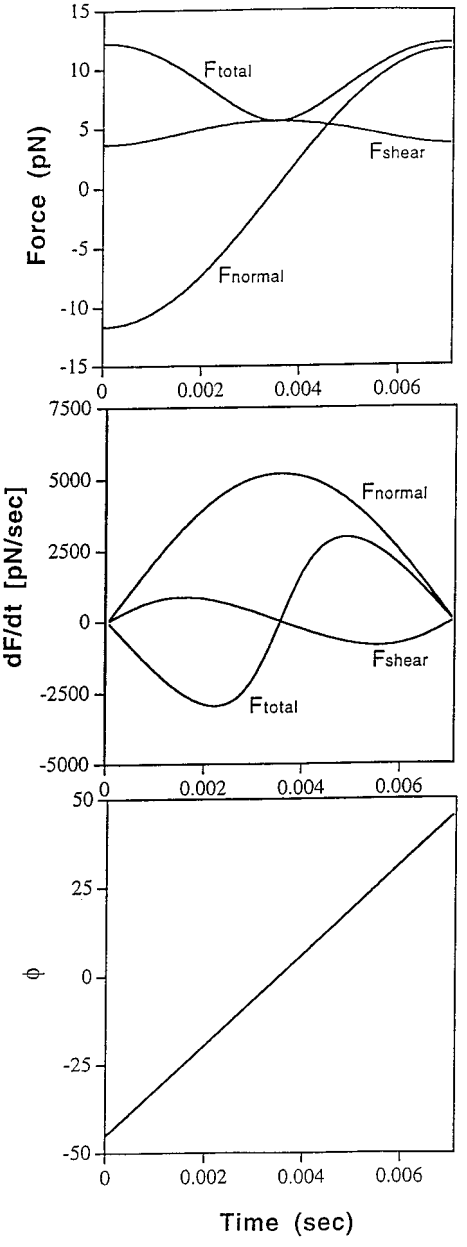

FIGURE 9 Hydrodynamic forces F_{shear}, F_{normal}, and F_{total} (A) and corresponding force loading rates dF/dt (B) for a doublet of equal sized neutrophil rotating from $\phi = -\pi/4$ to $\pi/4$ (C) in the $\theta = \bar{\theta}$ plane at G + 100 s^{-1}.

where the x component of the velocity v_x at the instant of contact is given as a function of V_r, V_θ, V_ϕ as

$$v_x = \sin \theta \sin \phi V_r + \cos \theta \sin \phi V_\theta + \cos \phi V_\phi \quad \text{at } \theta', \phi' \qquad \text{(A3)}$$

To calculate the swept contact area A_{coll}, a roughness on the order of Δr is associated with the aggregates (400 nm for singlets). The magnitude of the roughness dictates the initial contact area. The diameter of the contact area, D_c, and initial contact area, A_0, are calculated to be

$$D_c = 2(a_1 + \Delta r)\sin \theta_1 \quad \text{and} \quad A_0 = \pi\left(\frac{D_c}{2}\right)^2 \qquad \text{(A4)}$$

where

$$\theta_1 = \cos^{-1}\left[\frac{(a_1 + \Delta r)^2 + a_1(a_1 + 2a_1\lambda + 2\Delta r)}{2(a_1 + \Delta r)(a_1 + a_1\lambda + \Delta r)}\right] \quad \text{(A5)}$$

The contact area diameter, D_c, multiplied by the swept arc length, gives A_{coll} for collisions initiated at θ', ϕ' and completed at $\theta = 0$ for a primary collision:

$$A_{coll} = D_c a_1 \sqrt{(\cos\theta)^2 + (\sin\theta \sin\phi)^2}\, \tan^{-1}(\tan\theta \sin\phi) \quad \text{(A6)}$$

The authors thank their many colleagues for helpful discussions.

This work was supported by National Institutes of Health grant HL 56621 and National American Heart Association grant 96-6670. SLD is a recipient of the National Science Foundation National Young Investigator award, and PT is a recipient of a grant from the American Heart Association, Southeastern Pennsylvania Affiliate.

REFERENCES

Adler, P. M. 1981a. Heterocoagulation in shear flow. *J. Colloid Interface Sci.* 83:106–115.

Adler, P. M. 1981b. Interaction of unequal spheres. I. Hydrodynamic interactions: colloidal forces. *J. Colloid Interface Sci.* 84:461–473.

Alon, R., S. Chen, K. D. Puri, E. B. Finger, and T. A. Springer. 1997. The kinetics of L-selectin tethers and the mechanics of selectin mediated rolling. *J. Cell Biol.* 138:1169–1180.

Alon, R., D. A. Hammer, and T. A. Springer. 1995. Lifetime of the P-selectin-carbohydrate bond and tensile force in hydrodynamic strength. *Nature.* 374:539–542.

Bargatze, R. F., S. Kurk, E. C. Butcher, and M. A. Jutila. 1994. Neutrophils roll on adherent neutrophils bound to cytokine-induced endothelial cells via L-selectin on the rolling cells. *J. Exp. Med.* 180:1785–1792.

Batchelor, G. K., and J. T. Green. 1972. The hydrodynamic interaction of two small freely moving spheres in a linear flow field. *J. Fluid Mech.* 56:375–400.

Bell, D. N., S. Spain, and H. L. Goldsmith. 1989a. Adenosine diphosphate-induced aggregation of human platelets in flow through tubes. I. Measurement of concentration and size of single platelets and aggregates. *Biophys. J.* 56:817–828.

Bell, D. N., S. Spain, and H. L. Goldsmith. 1989b. Adenosine diphosphate-induced aggregation of human platelets in flow through tubes. II. Effect of shear rate, donor sex and ADP concentration. *Biophys. J.* 56: 829–843.

Bell, G. I. 1979. A theoretical model for adhesion between cells mediated by multivalent ligands. *Cell Biophys.* 1:133–147.

Bell, G. I. 1981. Estimate of the sticking probability for cells in uniform shear flow with adhesion caused by specific bonds. *Cell Biophys.* 3:289–304.

Belval, T. K., and J. D. Hellums. 1986. Analysis of shear induced platelet aggregation with population balance mathematics. *Biophys. J.* 50: 479–487.

Chang, H. N., and C. R. Robertson. 1976. Platelet aggregation by laminar shear and Brownian motion. *Ann. Biomed. Eng.* 4:151–183.

Chang, K. C., and D. A. Hammer. 1996. Influence of direction and type of applied force on the detachment of macromolecularly bound particles from surfaces. *Langmuir.* 12:2271–2282.

del Pozo, M. A., R. Pulido, C. Munoz, V. Alvarez, A. Humbria, M. R. Campareno, and F. Sanchez Madrid. 1994. Regulation of ICAM-3 (CD50) membrane expression on human neutrophils through a proteolytic shedding mechanism. *Eur. J. Immunol.* 24:2586–2594.

Dembo, M., D. C. Torney, K. Saxman, and D. Hammer. 1988. The reaction limited kinetics of membrane to surface adhesion and detachment. *Proc. R. Soc. Lond.* 234:55–83.

Diamond, M. S., and T. A. Springer. 1993. A subpopulation of Mac-1 (CD11b/CD18) molecules mediates neutrophil adhesion to ICAM-1 and fibrinogen. *J. Cell Biol.* 120:545–556.

Finger, E. B., K. D. Puri, R. Alon, M. B. Lawrence, U. H. von Andrian, and T. A. Springer. 1996. Adhesion through L-selectin requires a threshold hydrodynamic shear. *Nature.* 379:266–269.

Friedlander, S. K. 1977. Smoke, Dust and Haze: Fundamentals of Aerosol Behavior. Wiley, New York.

Goldsmith, H. L., O. Lichtarge, M. Tessier-Lavigne, and S. Samira. 1981. Some model experiments in hemodynamics. VI. Two-body collisions between blood cells. *Biorheology.* 18:531–555.

Granger, D. N., and G. W. Schmid-Schonbein. 1993. Physiology and Pathophysiology of Leukocyte Adhesion. Oxford University Press, New York.

Guyer, D. A., K. L. Moore, E. B. Lynam, C. M. Schmmel, S. Rogelj, R. P. McEver, L. K. Sklar. 1996. P-selectin glycoprotein ligand-1 (PSGL-1) is a ligand for L-selectin in neutrophil aggregation. *Blood.* 88:2415–2421.

Hammer, D. A., and H. Apte. 1992. Simulation of cell rolling and adhesion. *Biophys. J.* 63:36–57.

Huang, P. Y., and J. D. Hellums. 1993a. Aggregation and disaggregation kinetics of human blood platelets. Part I: development and validation of a population balance method. *Biophys. J.* 65:334–343.

Huang, P. Y., and J. D. Hellums. 1993b. Aggregation and disaggregation kinetics of human blood platelets. Part II: shear-induced platelet aggregation. *Biophys. J.* 65:344–353.

Huang, P. Y., and J. D. Hellums. 1993c. Aggregation and disaggregation kinetics of human blood platelets. Part III: disaggregation under shear stress of platelet aggregation. *Biophys. J.* 65:354–361.

Lauffenburger, D. A., and J. L. Linderman. 1993. Receptors: Models for Binding, Trafficking, and Signalling. Oxford University Press, New York.

Lawrence, M. B., G. S. Kansas, E. J. Kunkel, and K. Ley. 1997. Threshold levels of fluid shear promote leukocyte adhesion through selectins (CD62L, P, E). *J. Cell Biol.* 136:717–727.

Lawrence, M. B., and T. A. Springer. 1991. Leukocytes roll on a selectin at physiologic flow rates: distinction from and prerequisite for adhesion through integrins. *Cell.* 65:859–873.

Manley, R. J., and S. G. Mason. 1952. Particle motions in sheared suspensions. II. Collisions of uniform spheres. *J. Colloid Interface Sci.* 7:354–369.

Moore, K. L., A. Varki, and R. P. McEver. 1991. GMP-140 binds to a glycoprotein receptor on human neutrophils: evidence for a lectin-like interaction. *J. Cell Biol.* 112:491–499.

Neelamegham, S., A. D. Taylor, J. D. Hellums, M. Dembo, C. W. Smith, and C. I. Simon. 1997. Modeling the reversible kinetics of neutrophil aggregation under hydrodynamic shear. *Biophys. J.* 72:1527–1540.

Okuyama, M., J. Kambayashi, M. Sakon, and M. Monden. 1996. LFA-1/ICAM-3 mediates neutrophil homotypic aggregation under fluid shear stress. *J. Cell. Biochem.* 60:550–559.

Shao, J. Y., and R. M. Hochmuth. 1997. Mechanical anchoring strength of L-selectins and β_2-integrins to neutrophil cytoskeleton and membrane. *Ann. Biomed. Eng.* 25:200 (Abstr.).

Smith, M. J., C. L. Ramos, K. Ley, and M. B. Lawrence. 1997. Effect of shear force on lifetime of L-selectin bonds. *Ann. Biomed. Eng.* 25:198 (Abstr.).

Smoluchowski, M. V. 1917. Vensuch einer mathematischen theorie der koagulation kinetic kolloider losungen. *Z. Phys. Chem.* 92:129–168.

Swift, D. L., and S. K. Friedlander. 1964. The coagulation of hydrodols by Brownian motion and laminar shear flow. *J. Colloid Interface Sci.* 19:621–647.

Tandon, P., and S. L. Diamond. 1997. Hydrodynamic effects and receptor interactions of platelets and their aggregates in linear shear flow. *Biophys. J.* 73:2819–2835.

Taylor, A. D., S. Neelamegham, J. D. Hellums, C. W. Smith, and S. I. Simon. 1996. Molecular dynamics of the transition from L-selectin to β_2-integrin dependent neutrophil adhesion under defined hydrodynamic shear. *Biophys. J.* 71:3488–3500.

Tha, S. P., and H. L. Goldsmith. 1986. Interaction forces between red cells agglutinated by antibody. *Biophys. J.* 50:1109–1116.

Van de Ven, T. M. 1989. *Colloidal Hydrodynamics.* Academic Press, London.

Walchek, B., K. L. Moore, R. P. McEver, and T. K. Kishimoto. 1996. Neutrophil-neutrophil interactions under hydrodynamic shear stress involve L-selectin and PSGL-1. A mechanism that amplifies initial leukocyte accumulation of P-selectin in vitro. *J. Clin. Invest.* 98: 1081–1087.

Wang, H., A. Z. Zinchenko, and R. H. Davis. 1994. The collision rate of small drops in linear flow fields. *J. Fluid Mech.* 265:161–188.

Williams, M. M. R., and S. K. Loyalka. 1991. *Aerosol Science: Theory and Practice With Special Applications to the Nuclear Industry.* Pergamon Press, Tarrytown, NY.

Zeichner, G. R., and W. R. Schowalter. 1977. Use of trajectory analysis to study stability of colloidal dispersion in flow fields. *AIChE J.* 23: 243–254.